ORIGINAL ARTICLE

The recombinant bifunctional protein αCD133–GPVI promotes repair of the infarcted myocardium in mice

Y. BAUMER, *[1,2] C. LEDER, †[2] M. ZIEGLER, †[2] T. SCHÖNBERGER, † C. OCHMANN, † A. PERK, †
H. DEGEN, ‡ B. SCHMID-HORCH, ‡ M. ELVERS, § G. MÜNCH, ‡ M. UNGERER, † B. SCHLOSSHAUER* and
M. GAWAZ†

NMI, Natural and Medical Sciences Institute at the University of Tübingen, Regenerative Medicine I, Reutlingen; †University Clinic of Tübingen, Department of Internal Medicine III, Tübingen; ‡Corimmun GmbH, Martinsried; and §Institute for Clinical and Experimental Transfusion Medicine, Tübingen, Germany

Summary. *Background:* Bone-marrow-derived progenitor cells are important in myocardial repair mechanisms following prolonged ischemia. Cell-based therapy of diseased myocardium is limited by a low level of tissue engraftment. *Objectives:* The aim of this study was the development of the bifunctional protein αCD133–glycoprotein (GP)VI as an effective treatment for supporting vascular and myocardial repair mechanisms. *Results:* We have generated and characterized a bifunctional molecule (αCD133–GPVI) that binds both to the subendothelium of the injured microvasculature and to CD133^{+} progenitor cells with high affinity. αCD133–GPVI enhances progenitor cell adhesion to extracellular matrix proteins and differentiation into mature endothelial cells. In vivo studies showed that αCD133–GPVI favors adhesion of circulating progenitor cells to the injured vessel wall (intravital microscopy). Also, treatment of mice undergoing experimental myocardial infarction with αCD133–GPVI-labeled progenitor cells reduces infarction size and preserves myocardial function. *Conclusions:* The bifunctional trapping protein αCD133–GPVI represents a novel and promising therapeutic option for limiting heart failure of the ischemic myocardium.

Correspondence: Meinrad Gawaz, Department of Cardiology and Cardiovascular Diseases, Otfried-Müller Strasse 10, 72076 Tübingen, Germany.
Tel.: +49 7071 29 83688; fax: +49 7071 29 5040.
E-mail: meinrad.gawaz@med.uni-tuebingen.de

Correspondence: Burkhard Schlosshauer, Regenerative Medicine, NMI, Reutlingen, Germany.
Tel.: +49 7121 51530 20; fax: +49 7121 51530 16.
E-mail: schlosshauer@nmi.de

[1]Present address: Department of Medicine, University of Hawaii John A. Burns School of Medicine, Hawaii, USA.
[2]These authors contributed equally to this work.

Introduction

Myocardial repair is critical for the preservation of myocardial function following reperfusion after prolonged ischemia. Bone-marrow-derived progenitor cells (BMPCs) and endothelial progenitor cells (EPCs) can preserve myocardial function [1–5]; however, clinical studies evaluating cell-based therapy in myocardial infarction have shown variable and small effects [6–10]. The protective effects of BMPCs and EPCs on the myocardium following myocardial infarction appear to be related to the release of humoral factors and neovascularization [11]. One limiting effect of cell transplantation following myocardial infarction may be the low level of progenitor cell homing in the diseased myocardium [5]. EPCs, which express the surface antigen CD133, can differentiate into mature endothelial cells (ECs) and form new blood vessels [2]. Over 90% of human CD34^{+} cells in mobilized peripheral blood and human umbilical cord blood are also positive for CD133 [12].

Two major EPC populations are present in peripheral blood [13], early and late outgrowth EPCs [14]. Early EPCs have monocytic (CD45^{+} or CD14^{+}) and endothelial (CD31^{+}) characteristics; they show low CD34 expression and a low proliferation rate, but produce high levels of growth factors such as vascular endothelial growth factor (VEGF) and granulocyte colony-stimulating factor [13,15–18]. CD14^{+}/VEGF receptor (VEGFR)-2^{+}/CXCR2^{+} cells have been shown be incorporated into the denuded vessel wall and enhance endothelial recovery [19,20].

In contrast, late EPCs are endothelial colony-forming EPCs with high proliferation rates. These cells are non-monocytic (CD14^{−}) and express markers of mature ECs (CD31^{+}, VEFR-2^{+}, and Tie-2^{+}) [15,19]. These late EPCs are able to form tubular networks embedded in collagen gels [16,18]. However, both types of EPC, as well as other progenitor cell types (mesenchymal stem

cells and dendritic cells) [17,21], have been shown to have the potential to differentiate into mature ECs [12]. It is a very attractive proposition to locally and selectively trap these cells at sites of tissue injury in order to foster repair mechanisms.

Recently, we developed a chemically linked bifunctional guidance molecule, glycoprotein (GP)VI–CD133, that directs CD133$^+$ progenitor cells to sites of vascular lesions [22]. In vitro and in vivo, this construct substantially mediates EPC homing to vascular lesions [22].

Here, we describe and validate a fully recombinant bifunctional molecule, αCD133–GPVI, that preferentially binds to tissue lesions with destroyed vascular integrity and to CD133$^+$ cells. We constructed a recombinant bispecific molecule consisting of a single-chain mAb directed against human CD133 and a recombinant form of the soluble platelet collagen receptor GPVI that serves as an anchor structure to direct BMPCs to sites of vascular and myocardial damage. We found that administration of EPCs pretreated with αCD133–GPVI to mice during myocardial infarction significantly reduced infarction size (IS) and preserved ventricular function.

Materials and methods

Cloning and protein production

The cDNA sequences coding for the αCD133 single-chain fragment scFv-lh including a C-terminal strep-tag, for the scFv-lh–GPVI–FcIgG$_2$ fusion protein and the GPVI–FcIgG$_2$ control protein, were produced by gene synthesis and cloned into the mammalian expression vector pcDNA5-FRT via restriction sites *Hin*dIII and *Bam*HI (Geneart, Darmstadt, Germany). A Flp-In CHO cell line (Invitrogen, Carlsbad, CA, USA) was transiently transfected with the scFv-lh construct and stably transfected with either pcDNA5–scFv-lh–GPVI–FcIgG$_2$, pcDNA5–GPVI–FcIgG$_2$, or FcIgG$_2$, by the use of Lipofectamine 2000 transfection reagent (Invitrogen, Carlsbad, CA, USA), according to the manufacturer's protocol [23,24]. ScFv-lh-containing supernatant was harvested and purified by means of Strep-Tactin affinity purification (IBA BioTAGnology, Göttingen, Germany), according to the manufacturer's instructions. Stable cell lines were expanded with Ham's F12, 10% fetal bovine serum (FBS), 1% penicillin/streptomycin, and 500 μg mL^{-1} hygromycin B. For protein expression, cells were grown on T500 triple flasks in Ham's F12, supplemented with 2% FBS, which had been depleted of bovine IgG by protein-G affinity chromatography. Cellular supernatants were harvested 3–4 days after subculturing, and purified with 1-mL HITRAP Protein G HP columns (VWR, Darmstadt, Germany), according to the manufacturer's protocol.

Collagen-binding ELISA

The GPVI-binding capacity of produced proteins was tested with a collagen-binding ELISA. An Immulon 2 HB 96-well plate (Nunc, San Diego, CA, USA) was coated with 100 μL of 10 μg mL^{-1} bovine collagen I. 100 μl of either scFv-lh–GPVI–FcIgG$_2$ (αCD133–GPVI–FcIgG$_2$, in the following called αCD133–GPVI), GPVI–FcIgG$_2$ (in the following called GPVI) or FcIgG$_2$ (in the following called Fc) (range 5–1000 nM) was added. Subsequent procedures were carried out as described previously [23], and can be found in Data S1.

Competition assay

CD133$^+$ Weri-RB-1 cells (1.5×10^5) were analyzed by flow cytometry after incubation with competitive proteins (anti-CD133, αCD133–GPVI and GPVI at five different concentrations) and human anti-CD133/1 phycoerythrin (PE)-conjugated antibody (MACS; Miltenyi Biotec, Bergisch-Gladbach, Germany). All experiments were carried out with the corresponding PE-labeled IgG isotype control antibody (IgG isotype control; BD Biosciences, San Jose, CA, USA).

Western blot analysis with anti-IgG and anti-GPVI

Purified supernatant from αCD133–GPVI-producing cells was detected with western blot. The supernatant was prepared with reducing sample buffer, separated on a 10% SDS polyacrylamide gel, and transferred to a poly(vinylidene fluoride) membrane (Millipore, Billerica, MA, USA). The membrane was blocked with 5% powdered skimmed milk in phosphate-buffered saline with 0,5 % Tween (PBST), and probed with anti-IgG (peroxidase-conjugated AffiniPure goat anti-human IgG, Fc fragment-specific; Jackson ImmunoResearch, West Grove, PA, USA) at a dilution of 1 : 5000 and anti-GPVI (clone 5C4) at a dilution of 1 : 7500. Anti-GPVI was purified from the supernatant of hybridoma 5C4 [25]. The membrane was then incubated with fluorescence-labeled secondary antibodies in darkness. The membrane was detected with the Odyssey infrared imaging system (Licor, Bad Homburg, Germany).

Cells

Human CD34$^+$ cells were isolated from remnants of leukapheresis transplants, as described previously [26–28]. Experiments were approved by the local ethics committee of the University of Tübingen. Where indicated, we used control HEK293 cells or CD133-overexpressing HEK293 cells.

Multiple substrate array (MSA)

The MSA assay was carried out in ProPlate (Grace Bio-Labs, Bend, OR, USA) cultivation chambers mounted on microarray slides (Fig. S1C, upper panel). The wells were washed with PBS and coated differently (Data S1). Then, 1×10^5 human CD34$^+$ cells or 2×10^4 HEK cells were resuspended in appropriate culture medium (without FBS) and seeded in each culture chamber. The colonized microslides were kept at 37 °C and 5% CO$_2$ for 2 h (CD34$^+$ cells) or 30 min (HEK cells). Subsequent procedures were carried out as described previously [29].

Dynamic adhesion assay with a flow chamber

Control CD133-overexpressing HEK293 cells or human CD34$^+$ cells (1.5×10^5 cells mL^{-1}) were gently resuspended, transferred into a 50-mL syringe, and fixed in the perfusor. The shear rate was 2000 s^{-1} and the cell flow rate was 15 mL h^{-1} over the surfaces of precoated coverslips (coating; Data S1), which were fixed in the flow chamber. After 10 min, four movies of 30 s at different sites of the coverslip were recorded, and analyzed as previously described [26,27].

Colony-forming unit (CFU) assay

Human CD34$^+$ cells (5×10^4 cm^{-2}) were seeded in precoated 96-well plates (coating; Data S1) and cultivated at 37 °C and 5% CO$_2$ in EC growth medium MV2 (PromoCell, Germany). After 24 h, non-adherent cells were removed, and the medium was changed every 3 days. Additionally, endothelial CFUs were counted at days 1, 3, 5, 7, 10 and 14 by the use of light microscopy (Axiovert; Carl Zeiss, Oberkochen, Germany) [27,28].

Uptake of LDL DiI-Ac-LDL

Human CD34$^+$ cells (5×10^4 cm^{-2}) were seeded as described for the CFU assay. The uptake of DiI-Ac-LDL (Biomedical Technologies, Stoughton, MA, USA) of seeded CD34$^+$ cells was analyzed at days 1, 3, 5, 7, 10, and 14, as described previously [29].

Immunocytochemistry

Human CD34$^+$ cells (5×10^4 cm^{-2}) were seeded and analyzed as described for the CFU assay. HEK cells (2×10^4 cm^{-2}) were seeded onto uncovered wells and cultivated for 3 days. Immunocytochemistry was performed as described previously [29]. Staining of cells was performed with anti-CD133 (Abcam, Cambridge, UK), anti-CD34 (Abcam, Cambridge, UK), and VE-cadherin (Santa Cruz Biotechnologies, Santa Cruz, CA, USA). The actin cytoskeleton was visualized with Alexa-488-coupled phalloidin (Invitrogen, Darmstadt, Germany).

Assessment of CD34$^+$ adhesion with intravital fluorescence microscopy

Human CD34$^+$ cells were labeled with 5-carboxyfluorescein diacetate succinimidyl ester (Molecular Probes, Darmstadt, Germany) and incubated for 30 min with 20 µg mL^{-1} recombinant αGPVI–CD133 or GPVI (equimolecular). Intravital microscopy was performed as described previously [26–28,30] (see detailed description in Data S1). Fluorescent CD34$^+$ cells (5×10^4/250 µL) were injected intravenously into C57Bl/6J mice (Charles River, Sulzfeld, Germany). Before and after vascular injury of the carotid artery, interaction between CD34$^+$ cells and the vessel wall was visualized and quantified as described previously [31]. For intravital microscopy of the mesenteric vessels, segmental intestinal ischemia and reperfusion (I/R) was induced by ligation. Interaction between CD34$^+$ cells (preincubated with 10 µg mL^{-1} trapping protein or control [22]) and the vessel wall in arterioles and venules was recorded and quantified as described previously [32].

Myocardial I/R

Anesthesia and surgery were performed as described previously [33,34]. To induce myocardial infarction, left anterior descending artery (LAD) ligation was performed for 45 min in male NOD.CB17-Prkdc^{scid}/J mice (The Jackson Laboratory, Bar Harbor, MN, USA). Immediately and 3 days after surgery, the mice received 5×10^5 human CD34$^+$ cells per 250 µL via the tail vein, preincubated for 30 min with αCD133–GPVI (20 µg mL^{-1}), GPVI (equimolecular), or FcIgG$_2$ (equimolecular). An additional control group did not receive any cells. Seven days and 28 days after I/R, left ventricular function was assessed echocardiographically (Vevo 770; VisualSonics, Amsterdam, the Netherlands) by determination of the fractional area change (FAC). Reperfusion of the ischemic area (area at risk [AaR]) was estimated by Evans Blue/triphenyltetrazolium chloride (TTC) staining at days 1, 7, and 28. After religation of the left coronary artery at the level marked by the suture left in place, 4% Evans Blue was injected as a negative stain for perfused regions, and the infarcted area (IS) was determined by TTC staining (Sigma Aldrich, St. Louis, MO, USA). 1% TTC added to metabolically active tissue turns red; a white color indicates ischemic regions. The ISs were determined by quantitative morphometric planimetry, with an image analysis software program. The IS/AaR ratio indicates the size of damage/regeneration occurring in the heart after myocardial infarction [33,35].

Specific detection of injected human CD34$^+$ cells in the infarcted myocardium

Human CD34$^+$ cells (5×10^5) were resuspended in 250 µL of PBS and stained with PKH26-GL (Sigma-Aldrich, Darmstadt, Germany), according to the manufacturer's protocol. Cells were then incubated for 30 min with 10 µg g^{-1} body weight αCD133–GPVI or FcIgG$_2$ (equimolecular). Prepared CD34$^+$ cells were injected intravenously directly after transient LAD ligation. Human CD34$^+$ cells pretreated with αCD133–GPVI (10 µg g^{-1} body weight) were also injected intravenously into healthy control mice. Two hours after I/R, hearts were removed, cut in cryosections, stained with 4′,6-diamidino-2-phenylindole (Sigma-Aldrich, Darmstadt, Germany), and analyzed by immunofluorescence. The numbers of PKH26-GL-labeled human CD34$^+$ cells were quantified from 10 random cryosections of each heart sample ($n = 3$).

Immunohistochemistry

Paraffin-embedded cardiac sections taken 1 day after myocardial infarction were stained with hematoxylin and eosin,

according to a standard protocol. Immunostaining of infarcted cardiac sections was performed with a streptavidin–biotin–immunoperoxidase method (StreptABComplex/HRP, liquid diaminobenzidine, Substrate-Chromogen; Dako, Glostrup, Denmark). Paraffin-embedded cardiac sections taken on days 7 and 28 after I/R were stained with an anti-CD31 mAb (Santa Cruz Biotechnology, Santa Curz, CA, USA), cryosections taken 2 h after I/R were stained with an anti-IgG mAb (peroxidase-conjugated AffiniPure goat anti-human IgG, Fc fragment-specific; Jackson ImmunoResearch, West Grove, PA, USA), and paraffin-embedded cardiac sections taken day 1 after I/R were stained with an anti-Mac3 mAb (BD Biosciences, San Jose, CA, USA), an anti-polymorphonuclear (PMN) mAb (NIMP-R14; GeneTex, Irvine, CA, USA), and isotype control antibodies, according to a standard protocol. Corresponding secondary antibodies (Dako, Amsterdam, the Netherlands) were used. The percentages of Mac3-positive and PMN-positive cells were counted from six random areas in the infarcted myocardium of each heart sample ($n = 3$) in a blinded manner. The numbers of CD31-positive capillaries were quantified from six random areas from the infarction border zone of each heart sample ($n = 3$), and were referred to a certain tissue area (mm^2).

Statistics

All experiments were carried out more than three times in duplicate. Results are shown throughout as means ± standard errors of the mean. Statistical analysis was performed with PRISM (GraphPad Software, La Jolla, CA, USA), Student's *t*-test, and non-parametric Mann–Whitney test statistics. Statistical significance was set at $P < 0.05$.

Results

The recombinant bifunctional αCD133–GPVI protein displays functional binding sites

We designed and constructed two proteins, the bifunctional protein and a corresponding control protein. The bifunctional protein (termed trapping protein [Fig. 1A]; for sequences, see Fig. S1A) contains an anti-CD133 single-chain fragment
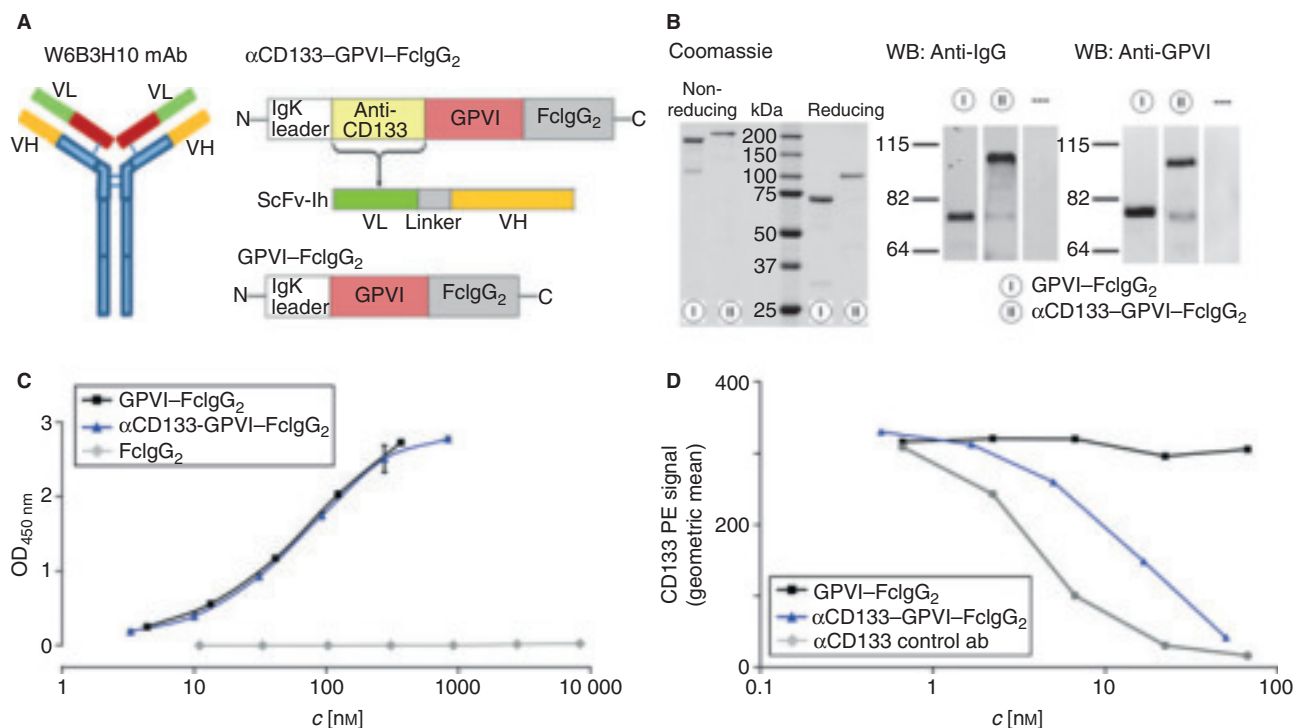

Fig. 1. In vitro characterization of αCD133–glycoprotein (GP)VI. (A) Construction of the fusion proteins. Both functional proteins contain a C-terminal-located FcIgG$_2$ domain (gray) followed by a functional GPVI collagen-binding domain (red). The N-terminus of each protein is formed by an IgK leader. In the trapping protein αCD133–GPVI–FcIgG$_2$, the functional anti-CD133 (αCD133)-binding domain (yellow) is positioned between the GPVI domain and the IgK leader. The αCD133-binding domain (ScFv-lh) consists of the variable regions of the anti-CD133 mAb W6B3H10 connected by an amino acid linker. (B) Western blot (WB) analysis. Stable protein-producing/secreting cells were generated. Proteins were purified from supernatants. Coomassie gel displayed the presence of protein dimers (non-reducing conditions) and monomers (reducing conditions). More detailed immunoblotting revealed, under reducing conditions, the IgG domain and GPVI domain at the predicted band sizes for both proteins. (C) Collagen binding. The GPVI-induced collagen-binding capacity of the constructed proteins was shown with a collagen-binding ELISA. Only the GPVI domain-containing proteins (trapping protein and GPVI–FcIgG$_2$) showed concentration-dependent collagen-binding qualities; FcIgG$_2$ did not. (D) CD133-binding assay. A CD133 competition assay using flow cytochemistry and αCD133 control antibody showed strong concentration-dependent neutralizing qualities. The use of the bifunctional recombinant trapping protein resulted in diminished but clearly detectable CD133-binding capacity, whereas the control protein GPVI–FcIgG$_2$ showed no CD133-binding potential. OD, optical density; PE, phycoerythrin; VH, heavy chain variable region; VL, light chain variable region.

(αCD133) to selectively home CD133-presenting progenitor cells out of the bloodstream to the injured tissue. This single-chain fragment consists of the variable regions of the anti-CD133 mAb W6B3H10 [36] connected by an amino acid linker with the sequence $(G_4S)_3$. Additionally, this recombinant bifunctional protein contains a GPVI domain for mediating high-affinity protein binding to collagen presented on disrupted endothelium, which was cloned and characterized [23,24,37]. We also developed a corresponding control protein not containing an αCD133 domain (Fig. 1A).

Both proteins were produced in cell culture and purified from cell supernatants. By western blot analysis aimed at IgG, we were able to demonstrate that supernatants contained the constructed proteins (Fig. 1B). Coomassie staining revealed that the proteins were expressed as dimers under non-reducing conditions (Fig. 1B). Under reducing conditions, monomers were present (Fig. 1B). Additionally, we showed that supernatants of GPVI-producing and trapping protein-producing cells showed western blot bands indicative of IgG (Fig. 1B, middle panel) and GPVI (Fig. 1B, right panel) at each predicted band size. Positively evaluated cell populations were expanded, and the proteins were purified from the corresponding supernatant.

In a second step, recombinant proteins were characterized with regard to their binding properties. The specificity of the GPVI-binding site was quantified with a collagen-binding assay (Fig. 1C). This ELISA-based method clearly demonstrated that both GPVI-containing proteins (monofunctional control and bifunctional protein) showed the same concentration-dependent collagen-binding efficiency, whereas an Fc negative control protein showed no collagen binding, indicating that the GPVI domain introduced into the proteins was functional. Next, we tested the αCD133-binding capacity of the recombinant bifunctional protein by performing a CD133 competition-based binding assay (Fig. 1D). Stable CD133-overexpressing (Weri-RB-1) cells were incubated with different concentrations of each protein construct or an αCD133-neutralizing antibody (W6B3H10) [22]. The CD133 expression levels on these preincubated cells were then analyzed by flow cytometry. Incubation of CD133-overexpressing cells with the GPVI protein revealed no effects on detectable CD133. In contrast, the neutralizing antibody (used as a positive control) showed a clear concentration-dependent decrease in detectable CD133 (Fig. 1D). Also, preincubation of CD133$^+$ cells with the trapping protein resulted in a concentration-dependent decrease in CD133, demonstrating that the novel recombinant trapping protein was functional and bound CD133 of CD133-expressing cells.

αCD133–GPVI enhances cell adhesion under static and dynamic conditions

To examine the bifunctional character of αCD133–GPVI, we used stable CD133-overexpressing HEK cells and human CD34$^+$ progenitor cells. Both cell types and the parent HEK^{CD133-} control cell line were examined for the expression of characteristic markers. In contrast to native HEK cells,

HEK^{CD133+} cells expressed CD133 but not CD34. CD34$^+$ cells served as a positive control, and displayed both CD133 and CD34 (Fig. S1C).

MSAs were employed to characterize cell attachment to extracellular matrix (ECM) proteins under static conditions (Fig. 2A,B; Fig. S1D). Fourteen different purified proteins (Fig. S1B) were microspotted onto nitrocellulose-coated glass slides (NMI TT, Germany) (spot size: 300 μm) [38]. Then, these spotted proteins were not coated (PBS) or coated (with GPVI or trapping protein), and subsequently incubated with different cell types (triple combination: ECM component–test protein–cell). All cell types showed attachment to poly(L-lysine) (positive control), whereas they did not adhere to serum albumin-coated surfaces (negative control). We could clearly detect enhanced cell attachment of CD133-expressing cells (Fig. 2A; Fig. S1D) specifically on trapping protein-coated ECM proteins (blue bars). Enhanced trapping protein-mediated cell attachment was evident on fibronectin, vitro-nectin, and collagens I–VI. Coatings with GPVI showed a similar background as with any other coating, indicating that enhanced attachment of exclusively CD133-expressing cells is mediated via an intact αCD133-binding site of the bifunctional protein. Essentially the same results were obtained when human CD34$^+$ progenitor cells were used (Fig. 2B; Fig. S1D). In summary, we demonstrated that the novel bifunctional protein is able to mediate enhanced and specific attachment of CD133$^+$ cells.

Besides these static adherence conditions, a dynamic paradigm was realized in flow chambers (Fig. 2C,D; Fig. S1E). Both native and CD133-overexpressing HEK cells were perfused over different coated surfaces under flow conditions. HEK^{CD133-} cells showed no adherence for all coatings (e.g. collagen coating: 1.25 ± 0.3 adherent cells per high-power field [HPF]). In contrast, HEK^{CD133+} cells strongly adhered when surfaces were coated with the bifunctional protein (16 ± 1.6 adherent cells per HPF) as compared with control protein GPVI (0.25 ± 0.3 adherent cells per HPF) or collagen (0 ± 0 adherent cells per HPF; Fig. 2C). Moreover, this effect was completely abolished by the addition of a soluble anti-CD133 antibody (1.25 ± 0.5 adherent cells per HPF). In addition, a strong increase in firm adhesion of CD34$^+$ progenitor cells was detected when surfaces were coated with the bifunctional protein (14.33 ± 4.0 adherent cells per HPF), and adherence was inhibited by a soluble anti-CD133 antibody (0.5 ± 0 adherent cells per HPF), similar to what was found for HEK^{CD133+} cells (Fig. 2D). These data strongly support the MSA findings.

αCD133–GPVI enhances endothelial differentiation of progenitor cells in vitro

Characterization of in vitro endothelialization was performed with CFU assays (Fig. 3A). Cultivation of progenitor cells on trapping protein-coated surfaces under endothelial medium conditions clearly resulted in faster and enhanced endothelial-like colony formation. Within the first 5 days in vitro, we
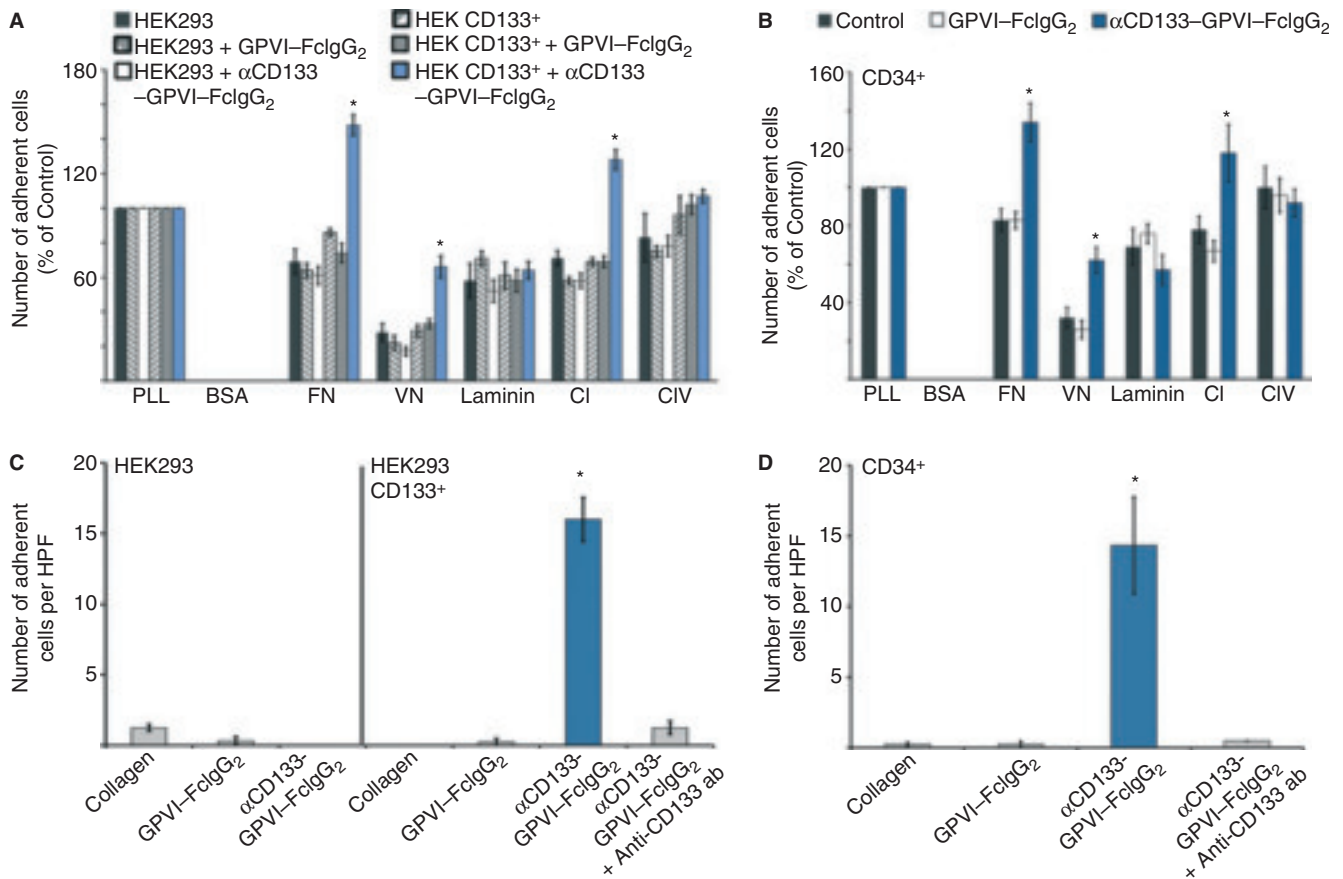
Fig. 2. In vitro bifunctionality of αCD133–glycoprotein (GP)VI. (A) Static adhesion. Static adhesion on different extracellular matrix proteins was tested with multisubstrate arrays (MSAs). Only cells expressing CD133 (HEK CD133 cells) showed enhanced adhesion to trapping protein-coated MSAs on fibronectin (FN), vitronectin (VN) and collagen type I (CI). The adhesion of added cells (independently of CD133 expression levels) was not modified when MSAs were uncoated or coated with GPVI–FcIgG$_2$. (B) Adhesion of human CD34$^+$ cells was analyzed with MSAs. CD34$^+$ cells showed significantly enhanced adhesion to αCD133–GPVI–FcIgG$_2$-coated MSAs on FN, VN, and collagen. (C) Dynamic adhesion experiments. These experiments revealed increased adhesion of only CD133$^+$ HEK293 cells on trapping protein-coated surfaces, which was abolished by a soluble anti-CD133 antibody. (D) Human CD34$^+$ cells showed increased adhesion on αCD133–GPVI–FcIgG$_2$-coated surfaces under flow conditions as compared to other coated surfaces. Adhesion was inhibited by a soluble anti-CD133 antibody. *P < 0.05. ab, antibody; BSA, bovine serum albumin; CIV, collagen IV; HPF, high-power field; PLL, Poly-L-Lysine.

detected three times as many colonies on trapping protein-coated surfaces (37 ± 3.6 colonies per 10^6 CD34$^+$ cells) as on uncoated ones (12 ± 2.6 colonies per 10^6 CD34$^+$ cells). This positive effect on CFU efficacy remained for up to 14 days in vitro (trapping protein, 68 ± 5.8 colonies per 10^6 CD34$^+$ cells; control, 37 ± 4.7 colonies per 10^6 CD34$^+$ cells), indicating a clear benefit for progenitor cells cultivated on the bifunctional protein.

These findings were substantiated by analysis of the uptake of DiI-labeled acetylated LDL (Fig. 3B; red fluorescence). Human CD34$^+$ progenitor cells cultivated on trapping protein-coated surfaces showed: (i) enhanced attachment of living cells (green calcein staining) (Fig. 3B, d as compared with a–c); and (ii) more rapid (day 5) and more efficient uptake of DiI-Ac-LDL (red fluorescence in Fig. 3B, l as compared with i–k). Moreover, these cells on trapping protein-coated surfaces had a more endothelial-like morphology (Fig. 3B, x as compared with u–w). These results support the hypothesis of enhanced endothelialization mediated by the trapping protein.

αCD133–GPVI augments progenitor cell adhesion in vivo and preserves myocardial function after infarction

To study the effect of αCD133–GPVI-mediated recruitment of progenitor cells in vivo, we performed intravital microscopy of injured murine carotid artery (Fig. 4A). αCD133–GPVI significantly increased the number of stably adherent progenitor cells at denuded vessels within 5 min after ligation (892 ± 81 adherent CD34$^+$ cells) as compared with GPVI-coated cells (633 ± 66 adherent CD34$^+$ cells, P < 0.05). We also performed intravital microscopy after mesenteric I/R (Fig. 4B). Again, preincubation of human CD34$^+$ cells with the trapping protein [22] resulted in increased adhesion 60 min after reperfusion as compared with control labeled cells (67.69 ± 10.10 adherent CD34$^+$ cells vs. 26.73 ± 5.89 adherent CD34$^+$ cells). These data support the in vitro findings of selective homing of progenitor cells mediated by αCD133–GPVI.

To assess the effects of αCD133–GPVI on myocardial infarction *in vivo*, we used a mouse model of myocardial
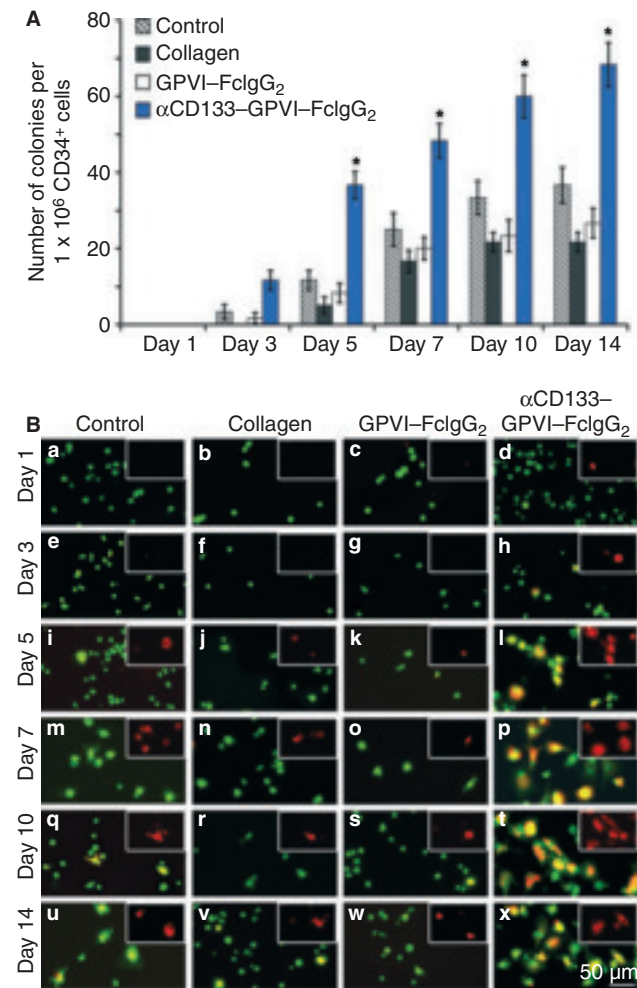
Fig. 3. *In vitro* endothelialization. Analysis by colony-forming unit assay (A) showed significantly enhanced endothelial colony formation of human $CD34^+$ cells when they were cultured on trapping protein-coated surfaces from day 5 onwards as compared with the other coatings. The number of adherent alive cells (calcein staining, green [B]) was increased on trapping protein-coated surfaces from the start onwards. The uptake of DiI-labeled acetylated LDL (DiI-Ac-LDL, red fluorescence [B]) of differentiating $CD34^+$ cells was increased on trapping protein-coated surfaces from day 5 onwards. Scale bar: 50 μm. *$P < 0.05$ indicates significant differences relative to control or glycoprotein (GP)VI–FcIgG$_2$-coated conditions. Error bars indicate standard error of the mean.

ischemia [33,34]. In this model, myocardial damage is assessed after LAD ligation for 45 min followed by reperfusion. NOD/Scid mice were given two administrations of human $CD34^+$ cells pretreated with αCD133–GPVI or control Fc, respectively (Fig. 4C). Twenty-eight days after reperfusion, infarction areas in αCD133–GPVI-treated mice, as assessed by TTC staining to differentiate between metabolically active and inactive tissue, were significantly reduced by up to 50% in comparison with mice treated with Fc control (IS/left ventricle, 15.8% ± 3% vs. 30.3% ± 2%, $P < 0.05$; IS/AaR, 29.6%% ± 6% vs. 46.6% ± 2%, $P < 0.05$; Fig. 4D). No significant differences were noted at day 1 and day 7 after transient ischemia between αCD133–GPVI and control Fc (Fig. 4D; control vs. αCD133–GPVI-treated mice, $P > 0.4$ at day 1, and $P > 0.07$ at day 7).

The reduction in IS was functionally relevant, because echocardiography 28 days after IS/R showed significantly improved cardiac left ventricular systolic function in mice treated with αCD133–GPVI as compared with Fc control-treated mice (FAC: 41.7% ± 3% vs. 30.5% ± 2%, $P < 0.05$; Fig. 4E and Video Clip S1). Again, no difference in left ventricular function was found at day 7 (Fig. 4E).

Total cell number and cell quality were analyzed by immunohistochemical staining 1 day after myocardial infarction. We found that, 1 day after myocardial infarction, the heart sections from mice treated with cells and protein (αCD133–GPVI or control protein) did not show a significant difference in total cell number. In contrast, 1 day after myocardial ischemia, mice without cell treatment showed a significantly lower total cell count than mice treated with cells (no cells vs. cell-treated mice, $P < 0.05$). At 7 days and 28 days after myocardial infarction, all groups showed equal total cell counts (Fig. 4F). In addition, we found increased numbers of macrophages (Mac3 staining, $P = 0.200$) and similar numbers of PMN cells (PMN staining, $P = 0.299$) in the infarcted myocardium in αCD133–GPVI-treated mice as compared with the control group 1 day after myocardial infarction (Fig. 4G).

Next, neovascularization in the infarct border zone was detected with a CD31 antibody. In the αCD133–GPVI-treated group, the average capillary density was enhanced at day 7 as compared with the FcIgG$_2$ control group by trend (599 ± 47 capillaries mm^{-2} vs. 487 ± 36 capillaries mm^{-2}, $P = 0.123$), and was significantly enhanced at day 28 after I/R (330 ± 14 capillaries mm^{-2} vs. 143 ± 24 capillaries mm^{-2}, $P = 0.002$; Fig. 4H).

Specific accumulation of αCD133–GPVI in the injured myocardium was shown by immunohistochemistry. We found enhanced αCD133–GPVI accumulation in the infarcted myocardium, especially around the blood vessels, 2 h after I/R as compared with control FcIgG$_2$ accumulation in the infarcted myocardium or αCD133–GPVI accumulation in the intact myocardium (Fig. 4I).

Human $CD34^+$ cells linked with PKH-26, and preincubated with αCD133–GPVI or control FcIgG$_2$, were specifically detected in the myocardium after 2 h. We found enhanced accumulation of human $CD34^+$ cells in the presence of αCD133–GPVI (59.0 ± 9.29 $CD34^+$ cells per 10 cryosections; Fig. 4J) compared to control FcIgG$_2$ (36.33 ± 9.21 $CD34^+$ cells per 10 cryosections), or control hearts (40.0 ± 8.01 $CD34^+$ cells per 10 cryosections). $P = 0.158$ indicates increased accumulation in the presence of αCD133–GPVI as compared with Fc control by trend.

Discussion

The major findings of the present study are as follows: (i) we generated a recombinant bifunctional αCD133–GPVI molecule that binds with high affinity to the CD133 antigen (single-chain anti-CD133) and to ECM proteins such as collagen and fibronectin (GPVI receptor); (ii) αCD133–GPVI augments adhesion of progenitor cells to ECM proteins and stimulates

differentiation into mature ECs; and (iii) the bifunctional molecule αCD133–GPVI augments adhesion of progenitor cells at sites of injured microvasculature in vivo, and improves neovascularization and preserves myocardial function after infarction in mice.

The findings imply that the bifunctional molecule αCD133–GPVI facilitates homing/entrapment of circulating progenitor cells at sites of myocardial injury, and thus favors repair mechanisms and preserves the function of infarcted myocardium. αCD133–GPVI-mediated progenitor cell adhesion may provide a novel strategy for the treatment of heart failure in patients with acute myocardial infarction.

Ischemia and subsequent reperfusion results in injury to the endothelial monolayer within the microvasculature of diseased myocardium [39]. The subendothelial matrix is exposed to the blood flow, resulting in platelet activation with subsequent enhanced platelet adhesion and accumulation of circulating blood cells such as monocytes and progenitor cells [39]. Since Asahara reported in 1997 that peripheral blood contains a small number of bone marrow-derived EPCs, it has been suggested that these cells could be used for myocardial repair and endothelial regeneration [40] and neovascularization [2]. Especially in the case of denuding injury, progenitor cells were reported to contribute to endothelial repair mechanisms [41,42]. Cell-based therapies for endothelial or myocardial repair are limited by low efficiency of engraftment to the target tissue and an unclear delivery system [43]. To improve myocardial engraftment of progenitor cells, we aimed to develop a single recombinant fusion protein that binds primarily to the injured microvasculature [22,23,37] and entraps circulating CD133$^+$ progenitor cells in the affected myocardium. We hypothesized that augmented enrichment of

CD133$^+$ progenitor cells within infarcted myocardium favors repair mechanisms.

Several subpopulations of EPCs with a diverse spectrum of marker expression have been reported to differentiate into mature endothelium and, in this way, to reconstitute the endothelial monolayer after injury. Bone marrow-derived CD34$^+$/VEGFR-2$^+$ monocytic cells were found to be embedded in newly formed blood vessels in ischemic tissue [40,44]. Additionally, EPCs positive for CD133 were shown to play a crucial role in regeneration of infarcted myocardium [45]. Under normal healthy conditions, the number of circulating EPCs is very low. However, acute tissue injury results in an increased number of circulating CD34$^+$ [46] as well as VEGFR-2$^+$/CD133$^+$ EPCs [47]. Ischemic tissue is known to produce chemokines such as stromal cell-derived factor-1 and VEGF, resulting in enhanced EPC mobilization and chemoattraction [48,49], and homing of EPCs to the subendothelial matrix [11,19,50]. Autologous administration of CD133$^+$ cells has been shown to improve the function of ischemic myocardium in humans [45]. A major limitation of cell-based therapy is, however, the low level of EPC entrapment within the diseased myocardium [50].

We constructed a bifunctional fusion protein that binds to ECM proteins of the injured subendothelium and also to the CD133 antigen of EPCs. We hypothesized that the 'anchor' molecule GPVI binds preferentially to the injured vasculature of the microcirculation, and thereby increases the accumulation of 'repair' cells [22]. Indeed, we found enhanced cell accumulation within the injured myocardium in mice treated with αCD133–GPVI (Fig. 4J) Furthermore, we provide in vitro and in vivo evidence that αCD133–GPVI augments progenitor cell adhesion to ECM proteins and promotes differentiation into

Fig. 4. In vivo characterization of αCD133–glycoprotein (GP)VI and effect on functional outcome after myocardial infarction (MI). (A) In C57BL/6J mice, 5-carboxyfluorescein diacetate succinimidyl ester (DCF)-stained human CD34$^+$ cells were injected intravenously, and the common carotid artery was injured by ligation [22]. Preincubation with αCD133–GPVI (20 µg mL^{-1}) led to significantly more cells adhering to the injured vessel wall than GPVI incubation. Scale bar: 50 µm. *P < 0.05, n = 6. The upper panel shows representative images of the lesion site 5 min and 30 min after injury. (B) In C57BL/6J mice, DCF-stained human CD34$^+$ cells were injected intravenously, and mesenteric ischemia/reperfusion was performed [32]. Preincubation with αCD133–GPVI (10 µg mL^{-1}) [22] led to significantly more cells adhering to the injured vessel wall in arterioles and venules 60 min after reperfusion than incubation with GPVI + αCD133. **P < 0.01, n = 5. (C) In NOD/Scid mice, MI was induced by temporary ligation of the left anterior descending artery [33]. After reperfusion, the mice received human CD34$^+$ cells that were pretreated with either αCD133–GPVI (20 µg mL^{-1}) or control Fc (equimolar). An additional group of mice received no cell treatment. The experimental protocol is shown in the time line. (D) One day, 7 days and 28 days after myocardial ischemia/reperfusion, the infarction size of the αCD133–GPVI-treated mice was determined. There were no significant differences between the cell-treated groups and the group without cells at day 1 (P > 0.4) and at day 7 (P > 0.07). At day 28, the infarction size was significantly reduced as compared with both control groups. Scale bar: 1 mm. *P < 0.05, **P < 0.01, n = 5–6. Representative Evans Blue-stained and triphenyltetrazolium chloride-stained myocardial sections are shown in the left panel. (E) This morphologic improvement was reflected by significantly better cardiac function 28 days after surgery, as assessed by echocardiography in vivo (right panel, *P < 0.05, **P < 0.01, n = 5–6). The left panel shows representative systolic and diastolic echocardiograms in long-axis view at day 28. (F) Murine cardiac sections were stained with hematoxylin and eosin (H&E). The left panel shows representative images. Scale bar: 100 µm. Magnification × 200. Quantitative analysis of H&E staining (right panel) showed an increase in total cell number after 1 day in mice treated with cells (αCD133–GPVI and control) as compared with mice without cell treatment (the difference between cell-treated groups and the group without cell treatment showed significance; *P < 0.05). At day 7 and day 28 after ischemia/reperfusion, there were similar total cell numbers. (G) Murine cardiac sections were immunostained for Mac3 and polymorphonuclear (PMN) cells. The upper panel shows representative images. Scale bar: 100 µm. Magnification: × 200. Quantitative analysis of immunostained sections showed increased numbers of Mac3-positive cells (P = 0.200) and similar numbers of PMN-positive cells (P = 0.299) in the infarcted myocardium. (H) Cardiac sections from mice were immunostained for CD31. Representative images (left panel) and quantitative analysis (right panel) showed enhanced neovascularization in the infarcted areas of αCD133–GPVI-treated mice as compared with the Fc control group. Scale bar: 50 µm. Magnification: × 200. There was no significance difference on day 7 (P = 0.123), but there was a significant difference on day 28 (P = 0.002). (I) Cardiac sections from mice 2 h after MI were immunostained for FcIgG$_2$ to detect the fusion protein αCD133–GPVI; representative images are shown. Scale bar: 50 µm. Magnification: × 200×. (J) Quantification of recruited human CD34$^+$ cells into the heart 2 h after ischemia/reperfusion. Accumulation of human CD34$^+$ cells preincubated with αCD133–GPVI was enhanced as compared with the FcIgG$_2$ control group by trend (P = 0.158). LV, left ventricular; FAC, fractional area change.

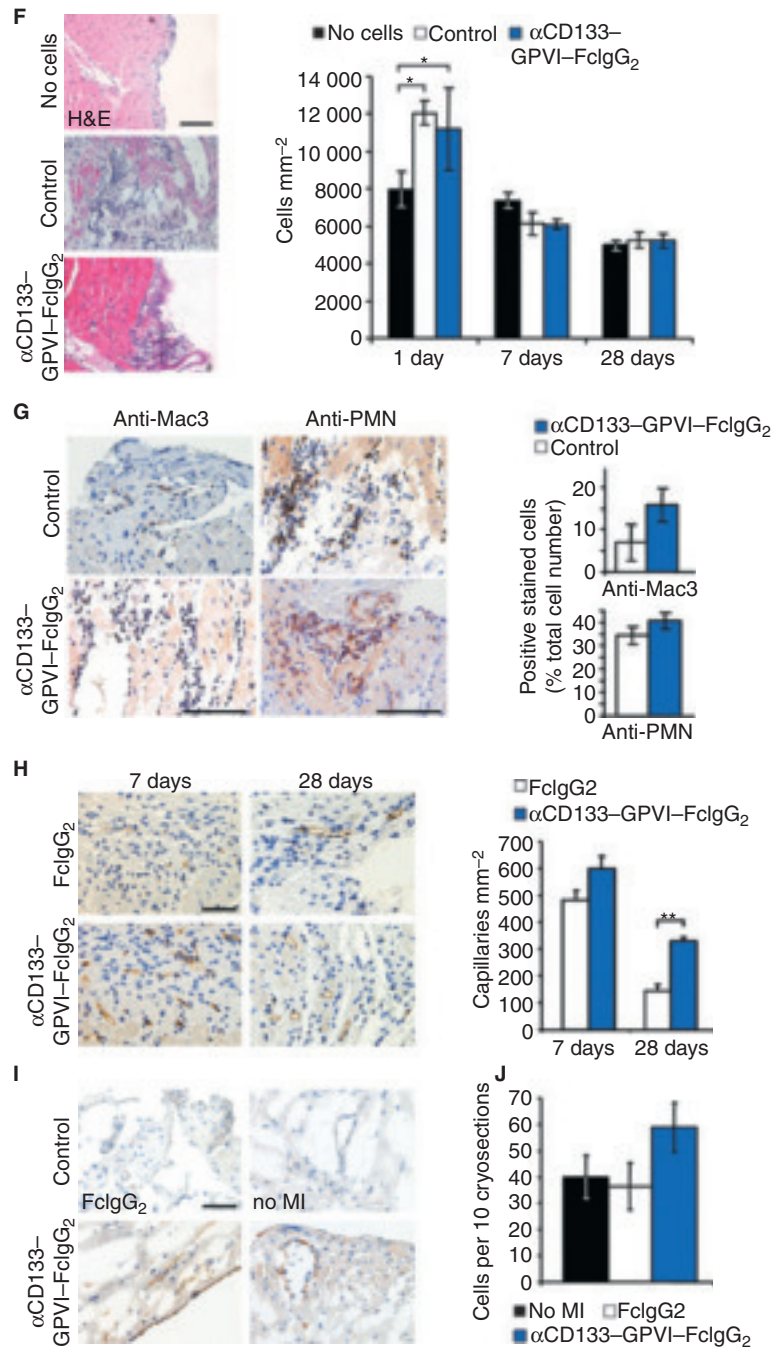© 2012 International Society on Thrombosis and Haemostasis
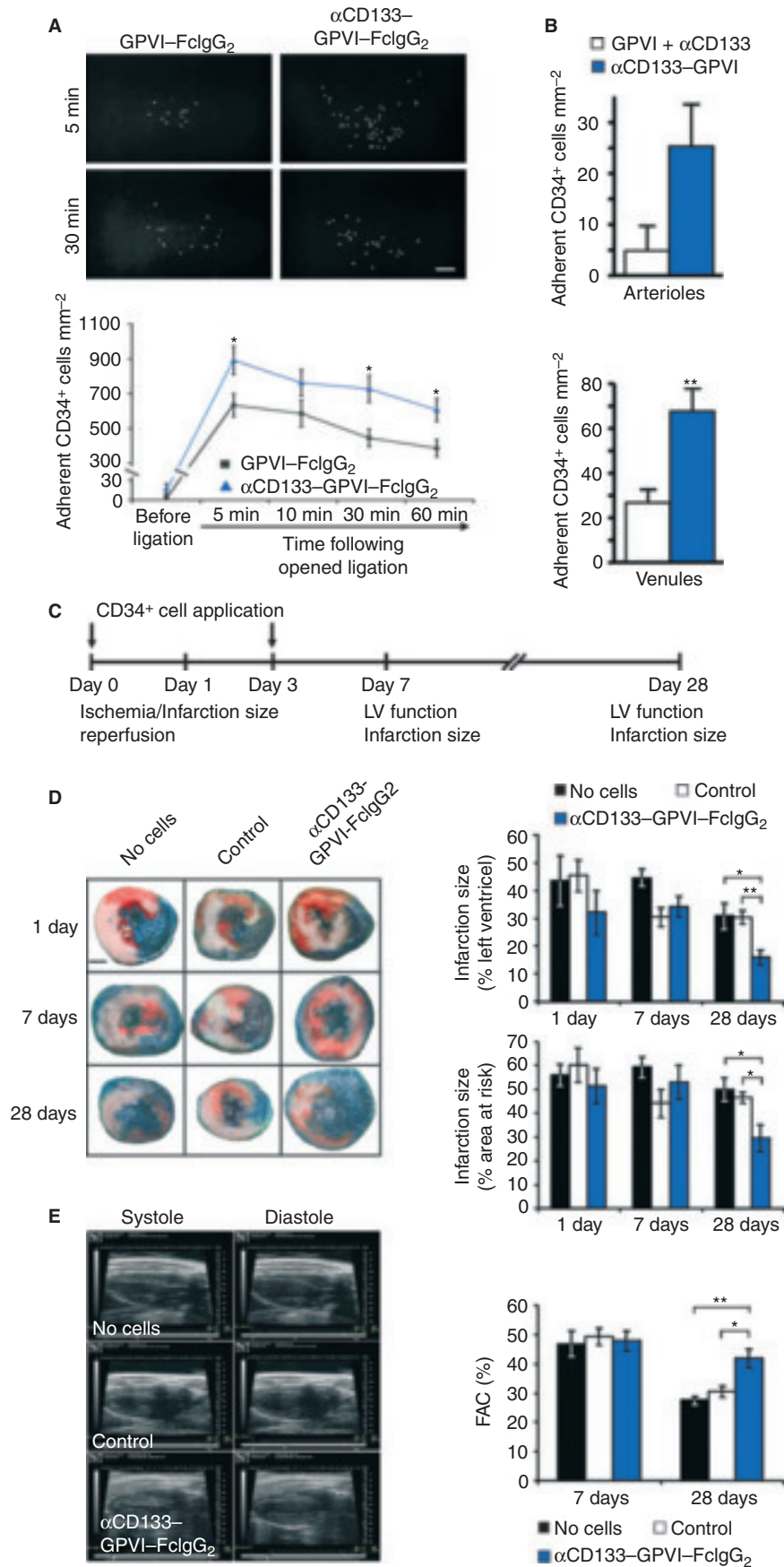
Fig. 4 Continued

mature endothelial cells. After transient myocardial ischemia (LAD ligation), systemic administration of human $CD34^+$ cells labeled with αCD133–GPVI significantly reduces IS and preserves myocardial function in mice (Fig. 4D,E). Although we were able to show that our transplanted CD133–GPVI-pretreated cells accumulate within the diseased myocardium, this seems to be less pronounced than shown by our intravital microscopy analysis. However, owing to the limitations of the two-dimensional histologic analysis, we might have underestimated the proportion of recruited cells.

Capture of circulating EPCs is an attractive approach to improve vascular and tissue healing after injury. In a different context, King *et al.* demonstrated that circulating hematopoietic stem and progenitor cells positive for CD34 are preferentially trapped under flow conditions when surfaces are coated with P-selectin [51]. Using the P-selectin approach seemed to be more effective with regard to $CD34^+$ cell homing than the use of anti-CD34 antibodies in microtubes [47]. Also, CD31-specific aptamers were developed to selectively recruit endothelial precursors to vascular grafts in a porcine in vitro model

[52]. All of these approaches have in common the fact that monofunctional capture molecules are coated onto different implant surfaces in order to endothelialize the technical devices. Recently, we have shown that a mAb directed against CD133 and chemically linked to the soluble collagen receptor GPVI augments vascular healing after carotid injury in mice [22]. In the present study, we show that pretreatment of progenitor cells with αCD133–GPVI may facilitate and improve cell transplantation in patients with myocardial infarction. Although not directly shown in the present study, it is tempting to speculate that systemic administration of αCD133–GPVI at the time of reperfusion of the infarction-related artery may be an alternative strategy to favor repair mechanisms of the infarcted myocardium.

In conclusion, we provide evidence that the bispecific molecule αCD133–GPVI is highly effective in preserving myocardial function after ischemia. Administration of αCD133–GPVI during reperfusion and thereafter might be a promising strategy for the treatment of myocardial infarction in order to promote myocardial repair and limit heart failure.

Addendum

Acknowledgements

Disclosure of conflict of interests

Supporting Information

Additional Supporting Information may be found in the online version of this article:

Fig. S1. Protein sequence of αCD133–GPVI, characterization of cells used for in vitro studies, static adhesion, and images of flow chamber experiments.
Fig. S2. Images of colony-forming unit assay of CD34$^+$ cells cultured on different coatings for 14 days with staining of the actin cytoskeleton.
Data S1. Methods.
Video Clip S1. Echocardiography 28 days after myocardial ischemia/reperfusion. Representative long-axis movies of one mouse per group are shown.

Please note: Wiley-Blackwell is not responsible for the content or functionality of any supporting materials supplied by the authors. Any queries (other than missing material) should be directed to the corresponding author for the article.

References

1 Christoforou N, Oskouei BN, Esteso P, Hill CM, Zimmet JM, Bian W, Bursac N, Leong KW, Hare JM, Gearhart JD. Implantation of mouse embryonic stem cell-derived cardiac progenitor cells preserves function of infarcted murine hearts. *PLoS ONE* 2010; **5**: e11536.

2 Kocher AA, Schuster MD, Szabolcs MJ, Takuma S, Burkhoff D, Wang J, Homma S, Edwards NM, Itescu S. Neovascularization of ischemic myocardium by human bone-marrow-derived angioblasts prevents cardiomyocyte apoptosis, reduces remodeling and improves cardiac function. *Nat Med* 2001; **7**: 430–6.

3 Matsuura K, Honda A, Nagai T, Fukushima N, Iwanaga K, Tokunaga M, Shimizu T, Okano T, Kasanuki H, Hagiwara N, Komuro I. Transplantation of cardiac progenitor cells ameliorates cardiac dysfunction after myocardial infarction in mice. *J Clin Invest* 2009; **119**: 2204–17.

4 Orlic D, Kajstura J, Chimenti S, Jakoniuk I, Anderson SM, Li B, Pickel J, McKay R, Nadal-Ginard B, Bodine DM, Leri A, Anversa P. Bone marrow cells regenerate infarcted myocardium. *Nature* 2001; **410**: 701–5.

5 Rafii S, Lyden D. Therapeutic stem and progenitor cell transplantation for organ vascularization and regeneration. *Nat Med* 2003; **9**: 702–12.

6 Assmus B, Schachinger V, Teupe C, Britten M, Lehmann R, Dobert N, Grunwald F, Aicher A, Urbich C, Martin H, Hoelzer D, Dimmeler S, Zeiher AM. Transplantation of Progenitor Cells and Regeneration Enhancement in Acute Myocardial Infarction (TOPCARE-AMI). *Circulation* 2002; **106**: 3009–17.

7 Lunde K, Solheim S, Aakhus S, Arnesen H, Abdelnoor M, Egeland T, Endresen K, Ilebekk A, Mangschau A, Fjeld JG, Smith HJ, Taraldsrud E, Grogaard HK, Bjornerheim R, Brekke M, Muller C, Hopp E, Ragnarsson A, Brinchmann JE, Forfang K. Intracoronary injection of mononuclear bone marrow cells in acute myocardial infarction. *N Engl J Med* 2006; **355**: 1199–209.

8 Meyer GP, Wollert KC, Lotz J, Pirr J, Rager U, Lippolt P, Hahn A, Fichtner S, Schaefer A, Arseniev L, Ganser A, Drexler H. Intracoronary bone marrow cell transfer after myocardial infarction: 5-year follow-up from the randomized-controlled BOOST trial. *Eur Heart J* 2009; **30**: 2978–84.

9 Schachinger V, Erbs S, Elsasser A, Haberbosch W, Hambrecht R, Holschermann H, Yu J, Corti R, Mathey DG, Hamm CW, Suselbeck T, Assmus B, Tonn T, Dimmeler S, Zeiher AM. Intracoronary bone marrow-derived progenitor cells in acute myocardial infarction. *N Engl J Med* 2006; **355**: 1210–21.

10 Wollert KC, Meyer GP, Lotz J, Ringes-Lichtenberg S, Lippolt P, Breidenbach C, Fichtner S, Korte T, Hornig B, Messinger D, Arseniev L, Hertenstein B, Ganser A, Drexler H. Intracoronary autologous

bone-marrow cell transfer after myocardial infarction: the BOOST randomised controlled clinical trial. *Lancet* 2004; **364**: 141–8.

11 Hristov M, Weber C. Endothelial progenitor cells in vascular repair and remodeling. *Pharmacol Res* 2008; **58**: 148–51.

12 Peichev M, Naiyer AJ, Pereira D, Zhu Z, Lane WJ, Williams M, Oz MC, Hicklin DJ, Witte L, Moore MA, Rafii S. Expression of VEGFR-2 and AC133 by circulating human CD34(+) cells identifies a population of functional endothelial precursors. *Blood* 2000; **95**: 952–8.

13 Rehman J, Li J, Orschell CM, March KL. Peripheral blood 'endo-thelial progenitor cells' are derived from monocyte/macrophages and secrete angiogenic growth factors. *Circulation* 2003; **107**: 1164–9.

14 Hirschi KK, Ingram DA, Yoder MC. Assessing identity, phenotype, and fate of endothelial progenitor cells. *Arterioscler Thromb Vasc Biol.* 2008; **28**: 1584–95.

15 Gulati R, Jevremovic D, Peterson TE, Chatterjee S, Shah V, Vile RG, Simari RD. Diverse origin and function of cells with endothelial phe-notype obtained from adult human blood. *Circ Res* 2003; **93**: 1023–5.

16 Ingram DA, Mead LE, Tanaka H, Meade V, Fenoglio A, Mortell K, Pollok K, Ferkowicz MJ, Gilley D, Yoder MC. Identification of a novel hierarchy of endothelial progenitor cells using human peripheral and umbilical cord blood. *Blood* 2004; **104**: 2752–60.

17 Mund JA, Ingram DA, Yoder MC, Case J. Endothelial progenitor cells and cardiovascular cell-based therapies. *Cytotherapy* 2009; **11**: 103–13.

18 Yoder MC, Mead LE, Prater D, Krier TR, Mroueh KN, Li F, Krasich R, Temm CJ, Prchal JT, Ingram DA. Redefining endothelial pro-genitor cells via clonal analysis and hematopoietic stem/progenitor cell principals. *Blood* 2007; **109**: 1801–9.

19 Hristov M, Zernecke A, Liehn EA, Weber C. Regulation of endo-thelial progenitor cell homing after arterial injury. *Thromb Haemost.* 2007; **98**: 274–7.

20 Hristov M, Zernecke A, Bidzhekov K, Liehn EA, Shagdarsuren E, Ludwig A, Weber C. Importance of CXC chemokine receptor 2 in the homing of human peripheral blood endothelial progenitor cells to sites of arterial injury. *Circ Res* 2007; **100**: 590–7.

21 Passier R, van Laake LW, Mummery CL. Stem-cell-based therapy and lessons from the heart. *Nature* 2008; **453**: 322–9.

22 Langer HF, von der Ruhr JW, Daub K, Schoenberger T, Stellos K, May AE, Schnell H, Gauss A, Hafner R, Lang P, Schumm M, Buhring HJ, Klingel K, Conrad S, Schaller M, van Zandvoort M, Jung G, Dimmeler S, Skutella T, Gawaz M. Capture of endothelial progenitor cells by a bispecific protein/monoclonal antibody molecule induces reendothelialization of vascular lesions. *J Mol Med* 2010; **88**: 687–99.

23 Massberg S, Konrad I, Bultmann A, Schulz C, Munch G, Peluso M, Lorenz M, Schneider S, Besta F, Muller I, Hu B, Langer H, Kremmer E, Rudelius M, Heinzmann U, Ungerer M, Gawaz M. Soluble gly-coprotein VI dimer inhibits platelet adhesion and aggregation to the injured vessel wall in vivo. *FASEB J.* 2004; **18**: 397–9.

24 Ungerer M, Rosport K, Bultmann A, Piechatzek R, Uhland K, Schlieper P, Gawaz M, Munch G. Novel antiplatelet drug revacept (Dimeric Glycoprotein VI-Fc) specifically and efficiently inhibited collagen-induced platelet aggregation without affecting general he-mostasis in humans. *Circulation* 2011; **123**: 1891–9.

25 Cabeza N, Li Z, Schulz C, Kremmer E, Massberg S, Bultmann A, Gawaz M. Surface expression of collagen receptor Fc receptor -gamma/glycoprotein VI is enhanced on platelets in type 2 diabetes and mediates release of CD40 ligand and activation of endothelial cells. *Diabetes* 2004; **53**: 2117–21.

26 Langer H, May AE, Daub K, Heinzmann U, Lang P, Schumm M, Vestweber D, Massberg S, Schonberger T, Pfisterer I, Hatzopoulos AK, Gawaz M. Adherent platelets recruit and induce differentiation of murine embryonic endothelial progenitor cells to mature endothelial cells in vitro. *Circ Res* 2006; **98**: E2–10.

27 Stellos K, Langer H, Daub K, Schoenberger T, Gauss A, Geisler T, Bigalke B, Mueller I, Schumm M, Schaefer I, Seizer P, Kraemer BF, Siegel-Axel D, May AE, Lindemann S, Gawaz M. Platelet-derived

stromal cell-derived factor-1 regulates adhesion and promotes differ-entiation of human CD34+ cells to endothelial progenitor cells. *Cir-culation* 2008; **117**: 206–15.

28 Stellos K, Langer H, Gnerlich S, Panagiota V, Paul A, Schonberger T, Ninci E, Menzel D, Mueller I, Bigalke B, Geisler T, Bultmann A, Lindemann S, Gawaz M. Junctional adhesion molecule A expressed on human CD34(+) cells promotes adhesion on vascular wall and differentiation into endothelial progenitor cells. *Arterioscler Thromb Vasc Biol* 2010; **30**: 1127–36.

29 Baumer Y, Funk D, Schlosshauer B. Does telomerase reverse trans-criptase induce functional de-differentiation of human endothelial cells?. *Cell Mol Life Sci* 2010; **67**: 2451–65.

30 Lonsdorf AS, Kramer BF, Fahrleitner M, Schonberger T, Gnerlich S, Ring S, Gehring S, Schneider SW, Kruhlak MJ, Meuth SG, Nieswandt B, Gawaz M, Enk AH, Langer HF. Engagement of alphaIIbbeta3 (GPIIb/IIIa) with alphanubeta3 integrin mediates interaction of mel-anoma cells with platelets: a connection to hematogenous metastasis. *J Biol Chem* 2012; **287**: 2168–78.

31 Massberg S, Konrad I, Schurzinger K, Lorenz M, Schneider S, Zohlnhoefer D, Hoppe K, Schiemann M, Kennerknecht E, Sauer S, Schulz C, Kerstan S, Rudelius M, Seidl S, Sorge F, Langer H, Peluso M, Goyal P, Vestweber D, Emambokus NR, *et al.* Platelets secrete stromal cell-derived factor 1alpha and recruit bone marrow-derived progenitor cells to arterial thrombi in vivo. *J Exp Med* 2006; **203**: 1221–33.

32 Massberg S, Enders G, Leiderer R, Eisenmenger S, Vestweber D, Krombach F, Messmer K. Platelet–endothelial cell interactions during ischemia/reperfusion: the role of P-selectin. *Blood* 1998; **92**: 507–15.

33 Seizer P, Ochmann C, Schonberger T, Zach S, Rose M, Borst O, Klingel K, Kandolf R, Macdonald HR, Nowak RA, Engelhardt S, Lang F, Gawaz M, May AE. Disrupting the extracellular matrix metalloproteinase inducer–cyclophilin A interaction reduces infarct size and preserves systolic function after myocardial ischemia and reperfusion. *Arterioscler Thromb Vasc Biol* 2011; **31**: 1377–86.

34 Weig HJ, Bott-Flugel L, Stadele C, Winter K, Schmidt R, Gawaz M, Laugwitz KL, Seyfarth M. Impaired platelet function reduces myo-cardial infarct size in Galphaq knock-out mice in vivo. *J Mol Cell Cardiol* 2008; **44**: 143–50.

35 Borst O, Ochmann C, Schonberger T, Jacoby C, Stellos K, Seizer P, Flogel U, Lang F, Gawaz M. Methods employed for induction and analysis of experimental myocardial infarction in mice. *Cell Physiol Biochem* 2011; **28**: 1–12.

36 Bühring H, Marxer A, Lammers R, Wissinger B. In: *Leucocyte Typing VII. White Cell Differentiation Antigens. CD133 cluster report.* Oxford: Oxford University Press, 2002: 622–3.

37 Schonberger T, Siegel-Axel D, Bussl R, Richter S, Judenhofer MS, Haubner R, Reischl G, Klingel K, Munch G, Seizer P, Pichler BJ, Gawaz M. The immunoadhesin glycoprotein VI-Fc regulates arterial remodelling after mechanical injury in ApoE–/– mice. *Cardiovasc Res* 2008; **80**: 131–7.

38 Kuschel C, Steuer H, Maurer AN, Kanzok B, Stoop R, Angres B. Cell adhesion profiling using extracellular matrix protein microarrays. *Biotechniques* 2006; **40**: 523–31.

39 Gawaz M. Role of platelets in coronary thrombosis and reperfusion of ischemic myocardium. *Cardiovasc Res* 2004; **61**: 498–511.

40 Asahara T, Murohara T, Sullivan A, Silver M, van der Zee R, Li T, Witzenbichler B, Schatteman G, Isner JM. Isolation of puta-tive progenitor endothelial cells for angiogenesis. *Science* 1997; **275**: 964–7.

41 Hill JM, Zalos G, Halcox JP, Schenke WH, Waclawiw MA, Quyyumi AA, Finkel T. Circulating endothelial progenitor cells, vascular func-tion, and cardiovascular risk. *N Engl J Med* 2003; **348**: 593–600.

42 Walter DH, Rittig K, Bahlmann FH, Kirchmair R, Silver M, Murayama T, Nishimura H, Losordo DW, Asahara T, Isner JM. Statin therapy accelerates reendothelialization: a novel effect involving mobilization and incorporation of bone marrow-derived endothelial progenitor cells. *Circulation* 2002; **105**: 3017–24.

43 Chien KR. Regenerative medicine and human models of human disease. *Nature* 2008; **453**: 302–5.

44 Takahashi T, Kalka C, Masuda H, Chen D, Silver M, Kearney M, Magner M, Isner JM, Asahara T. Ischemia- and cytokine-induced mobilization of bone marrow-derived endothelial progenitor cells for neovascularization. *Nat Med* 1999; **5**: 434–8.

45 Stamm C, Westphal B, Kleine HD, Petzsch M, Kittner C, Klinge H, Schumichen C, Nienaber CA, Freund M, Steinhoff G. Autologous bone-marrow stem-cell transplantation for myocardial regeneration. *Lancet* 2003; **361**: 45–6.

46 Shintani S, Murohara T, Ikeda H, Ueno T, Honma T, Katoh A, Sasaki K, Shimada T, Oike Y, Imaizumi T. Mobilization of endothelial progenitor cells in patients with acute myocardial infarction. *Circulation* 2001; **103**: 2776–9.

47 Gill M, Dias S, Hattori K, Rivera ML, Hicklin D, Witte L, Girardi L, Yurt R, Himel H, Rafii S. Vascular trauma induces rapid but transient mobilization of VEGFR2(+)AC133(+) endothelial precursor cells. *Circ Res* 2001; **88**: 167–74.

48 Asahara T, Takahashi T, Masuda H, Kalka C, Chen D, Iwaguro H, Inai Y, Silver M, Isner JM. VEGF contributes to postnatal neovascularization by mobilizing bone marrow-derived endothelial progenitor cells. *EMBO J* 1999; **18**: 3964–72.

49 Ceradini DJ, Kulkarni AR, Callaghan MJ, Tepper OM, Bastidas N, Kleinman ME, Capla JM, Galiano RD, Levine JP, Gurtner GC. Progenitor cell trafficking is regulated by hypoxic gradients through HIF-1 induction of SDF-1. *Nat Med* 2004; **10**: 858–64.

50 Chavakis E, Urbich C, Dimmeler S. Homing and engraftment of progenitor cells: a prerequisite for cell therapy. *J Mol Cell Cardiol* 2008; **45**: 514–22.

51 Wojciechowski JC, Narasipura SD, Charles N, Mickelsen D, Rana K, Blair ML, King MR. Capture and enrichment of CD34-positive haematopoietic stem and progenitor cells from blood circulation using P-selectin in an implantable device. *Br J Haematol* 2008; **140**: 673–81.

52 Hoffmann J, Paul A, Harwardt M, Groll J, Reeswinkel T, Klee D, Moeller M, Fischer H, Walker T, Greiner T, Ziemer G, Wendel HP. Immobilized DNA aptamers used as potent attractors for porcine endothelial precursor cells. *J Biomed Mater Res A* 2008; **84**: 614–21.